Green synthesis of lead oxide nanoparticles, characterization and adsorption study for removal of malachite green dye

Abstract:

In this study lead oxide nanoparticles were synthesized by using ecofriendly and non-toxic Morus rubra extract. The obtained lead oxide nanoparticles were characterized by XRD, SEM, EDX, BET and FTIR techniques. Powder X-ray diffraction analysis revealed that synthesized PbO nanoparticles had crystallite structure of high purity. SEM survey shows that the obtained nanoparticles having in general uniform particle distribution and the particle sizes vary within the range of 22.4 to 29.2nm. As established by EDX to confirm the presence of lead and oxygen, the weight percentage of the latter was (71.5 % Pb and 28.5% O), respectively. FT-IR spectra exhibit a sharp peak at 439.38 and 595.46 cm^{-1} attributed to PbO vibration, confirming the formation of PbO nanoparticles. The effectiveness of MgO nanostructures for removing indigo carmine (IC) dye from an aqueous solution is demonstrated in this article. , the IC dye uptake and adsorption processes were investigated using a MgO sorbent. The maximum adsorption capacity and contact time were optimized which corresponding to 41.3 mg. g^{-1} and 60min respectively.

Keywords: Morus rubra extract, PbO nanoparticles, MG dye removal, Adsorption, contact time.

1. Introduction:

Nanotechnology and nanobiotechnology are advancing extremely quickly, particularly in the field of nanoparticle synthesis[1, 2]. Nanotechnology is now used as a crossover technology in electrical appliances[3], building[4], and composite materials[5], as well as consumer products[6]. Nanostructures have received a great deal of attention due to their small size and high surface-to-volume ratio, and their physicochemical properties can be distinguished from those of bulk materials[7-10]. Metal oxide nanoparticles are a promising tool for biomedical applications due to their high stability, simple manufacturing techniques, porosity, and their ability to be easily incorporated into hydrophobic and hydrophilic systems due to their negatively charged surface[11-13].

Lead oxide (PbO) is a significant industrial substance that has been widely used in batteries[14], pigments[15], and the glass industry[14]. They are widely used in construction skeletons, and road construction due to their anti-rust, anti-bacterial, and anti-algal characteristics[16-18]. Litharge (tetragonal crystalline structure) and massicot (orthorhombic crystalline structure) are the two crystalline forms of the semiconductor PbO[19, 20]. The -PbO form of litharge crystals has been demonstrated to be stable at low temperatures, whereas the -PbO form of massicot crystals appears to be stable at high temperatures[21, 22]. PbO nanostructures were manufactured utilizing multiple techniques, including thermal breakdown[23, 24], Sol–gel pyrolysis[21, 25], thermal decomposition under microwave radiation[16, 26], chemical deposition[16, 27], and solvothermal method[28].

Since lead pollution has a significant influence on the ecosystem, it is necessary to identify solutions. Metal oxide nanoparticles may be manufactured through nanotechnology and biosynthesis[29, 30]. Biosynthesis of nano-sized lead oxide (PbO-NPs) could improve its qualities while minimizing the number of harmful compounds used in its synthesis[31, 32]. In this study, PbO-NPs were synthesized utilizing Morus rubra extract, and the effect of preparation method on malachite green dye adsorption was examined.

2. Experimental methods

2.1 Synthesis of PbO-NPs

PbO-NPs were bio generated by applying Morus leaf extract as covering agents. 4.0 g of Morus leaves was weighed and washed with distilled water, then added to 100 ml of distilled water and left to boil for 15 minutes, then filtered, and the suspension was placed in a water bath at a temperature of 65 ° C for 120 minutes until a clear and yellow solution was induced. Then 5g of Pb $(NO_3)_2$ was slowly added to the solution (and stirred in a water bath at 80 °C, until a lemon-colored resin was formed. The resulting resin was dried in an oven at 90°C for 2 hours and then roasted at 500°C for 90 minutes. The result was observed to be an orange powder, known as PbO-NPs.

2.2 Adsorption studies:

All adsorption investigations were conducted with malachite green (MG) as the reference dye. MG is basically a cationic dye classed as a triarylmethane chloride dye. 4-4-dimethylaminophenyl-phenylmethylidene-1-cyclohexa-2,5-dienylidene-dimethyl

azanium chloride is its IUPAC designation. $\{C_6H_5\ [CC_6H_4]\ (CH_3)_2\}Cl$ having a molar mass of 327. The intense blue color of the dye is due to its strong absorption in visible region at 618 nm. In order to prevent photolysis, batch adsorption operations were conducted in foil-lined glass beakers using a magnetic stirrer (350 rpm) at room temperature. The standard concentration of malachite green was determined to be 10 ppm, from which various aliquots of the experimental sample were obtained. Before and after each experiment, the concentration of malachite green was evaluated by measuring the absorbance in the visible area with a UV–Vis absorption spectrophotometer. The quantity of IC adsorbed per gram of nanoparticles at time (min) can be calculated by the following equation (1).

$$qt = (C0 - Ct)\frac{V}{m}$$

Where C_0 and C_t are the initial and equilibrium concentrations of the dye, V is the dye solution volume, and m is the adsorbent's mass.

2.3 Characterization of PbO NPs:

PbO nanoparticles obtained was characterized using x-ray diffraction (XRD), energy dispersive x-ray(EDX),scanning electron microscopy (SEM) UV– Visible spectrometer, Brunauer Emmett Teller analyzer (BET)and Fourier transform infrared spectroscopy (FT-IR).Muffle furnace was used for calcination purposes, the phase structure and average crystallite size of the PbO-NPs nanoparticles were investigated by examining the powder's XRD patterns. The samples were recorded with a diffractometer (D8 Advance Bruker,Mannheim, Germany) using Cu–Kα radiation (λ = 0.15406 nm). The structural morphology and chemical composition of PbO nanoparticles were examined and measured by SEM – EDX. The specimens were previously oven-dried at 105 °C and coated with a thin film of gold to create electrical conduction on the surface of the PbO-powder. The mode of chemical bonding in the prepared samples was studied by FTIR (Nicolet 6700, The mode Fisher, Waltham, MA, USA) in the range of 4000–400 cm^{-1} with a resolution of 4 cm^{-1}.The samples' porosity was determined using N_2 adsorption-desorption isotherms at the N_2 boiling point (77 K) in ASAP 2020 (Micromeritics) equipment. Before the adsorption experiment, the specimen was degassed with Helium for two hours at 250 ^{o} C to remove moisture and adsorbed contaminants. The BET (Brunauer, Emmett and Teller) formula and the t-plot method of Lippens and de Boer were used to estimate the porosity and surface area.

3. Results and discussions

3.1 Scanning electron microscopy (SEM)

The size shape and rearrangement of the product PbO nanoparticles has been investigated by scanning electron microscopy (SEM). The SEM image of the synthesized nanoparticles has displayed that the particles are in nanoscale and uniform in shape. The particle size observed in the SEM image is in the range of 22.4-29.2 nm, which is good agreement with this estimator.

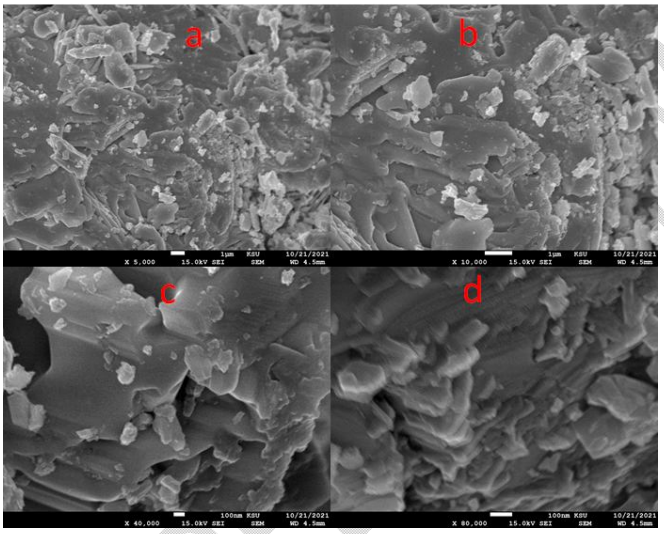

Figure (1): SEM image of PbO nanoparticles at different magnification

3.2 Energy dispersive x-ray spectra (EDX)

The EDX analysis was carried out for PbO - NPs at 15keV. Results revealed the presence of Lead (Pb) and oxygen (O) elements in PbO-NPs. The weight percent of Lead and oxide calculated from EDX analysis were O: 28.5 weight % and Pb: 71.5 weight %, respectively. There were no other elemental impurities in the EDX spectra. The EDX result showed the presence of uniform distribution of Lead to oxygen with atomic ratio of 3:1 in PbO. This result confirmed the formation of pure PbO-NPs. The elemental analysis of the sample shows that the prepared sample was Lead oxide.

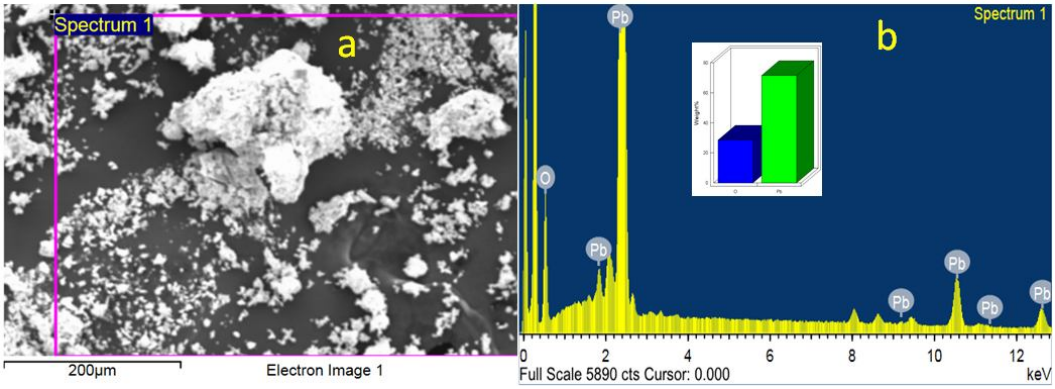

Figure (2): (a) FE-SEM of PbO NPs (b) EDX analysis and percent composition of PbO nanoparticles

3.3 X-ray diffraction (XRD)

The structural of the powder material is analyzed by X-Ray diffraction are showed in fig. (3). The obtained XRD results are compared to the JCPDS card. Here Fig.5 shows prominent peak of 2θ, this value is assigned to the plane (1 1 1) which indicates high crystalline nature of PbO.

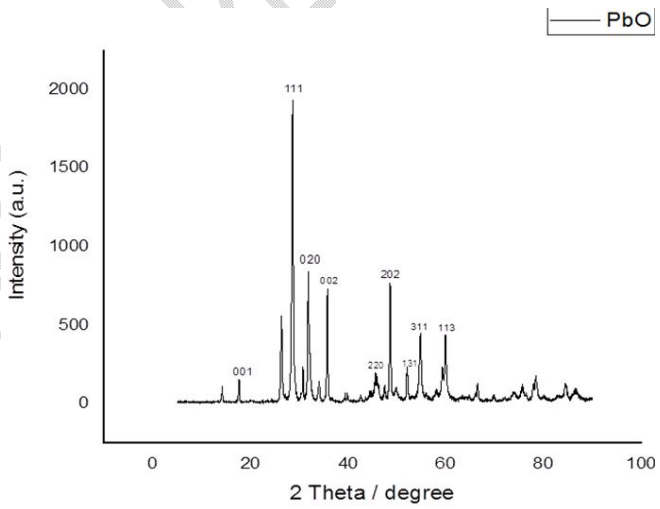

Figure (3): XRD analysis of PbO nanoparticles

3.4 Functional group analysis (IR)

Functional group analysis FTIR transmission spectra of PbO-NPs nanoparticles synthesized by precipitation method are shown in Fig.4. FTIR spectra were recorded

in solid phase using the KBr pellet technique in the range of 4000-400 cm^{-1}. FTIR analysis of green synthesized PbO - NPs revealed peaks at 429.42 and 530.21 cm^{-1} which can be attributed to vibrations of PbO - NPs, confirming the formation of highly pure PbO-NPs nanoparticles. The sharp peak observed at 1384.25 cm^{-1} is attributed to Pb-O stretching vibrations. The band around 3444.26 cm^{-1} show the presence of - OH stretching of hydroxyl groups due to moisture.

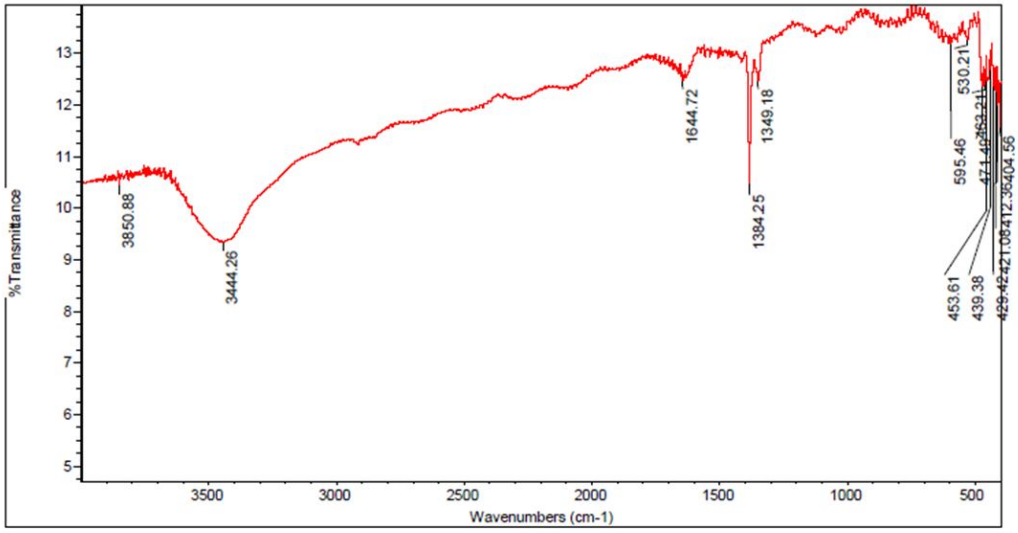

Figure (4): IR spectrum of PbO nanoparticles

3.5 The surface area (BET):

Nanomaterials can be identified by their specific surface area, which is one of the primary indicators of their nanoparticle content. PbO NPs were characterized by their surface area (BET). The approach is based on constant-temperature single-gas adsorption. As an adsorbate on the surface of PbO NPs, nitrogen gas was utilized. To assess the surface texture parameters of PbO, Brunauer Emmett Teller (BET) and Barrett Joyner Halenda (BJH) diagrams were utilized. Based on the N_2 sorption isotherm, the isotherm is of Langmuir type IV (Fig. 6a), with a relative pressure (P/Po = 0.0-0.99). In addition, the hysteresis loop is type H3 (Fig. 6b), confirming that the nanoparticles with slit-shaped pores are mesoporous. The results indicate that PbO NPs have a surface area of 2.975m^2/g, which is a considerable value. In addition, the pore volume and radius are 0.007 cc/g and 15.934A^0, respectively.

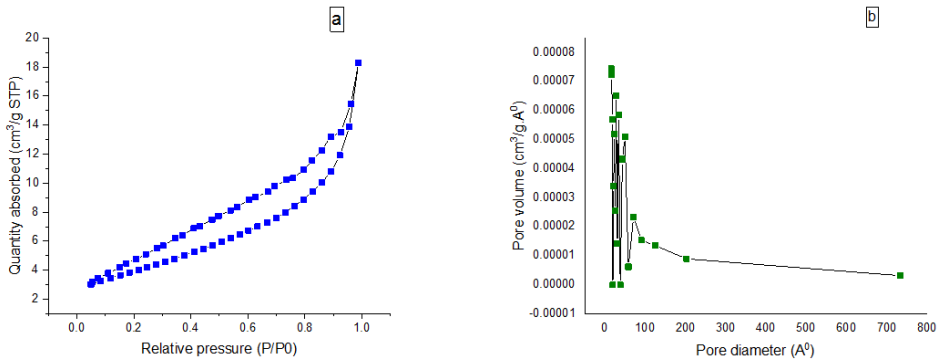

Figure (5): (a) (BET) and N_2 adsorption –desorption isotherm (b) (BJH) pore size distribution of the PbO nanoparticles sample

3.6 Adsorption study and contact time

Lead oxide nanocomposites were utilized as an adsorbent to evaluate MG adsorption. Equilibrium contact time is one of most significant parameters affecting the design of contaminated water treatment system. The effect of equilibrium time on MG dye adsorption was demonstrated in Fig.7. It can be noted that, the adsorption was rapid in the early stages of the adsorption process up to it gradually approached an equilibrium. The contact time and equilibrium adsorption capacity qe was about 60 min and 41.3mg/g in the MG dye concentration of 10 ppm, and short adsorption equilibrium time is useful for the quick adsorption application.

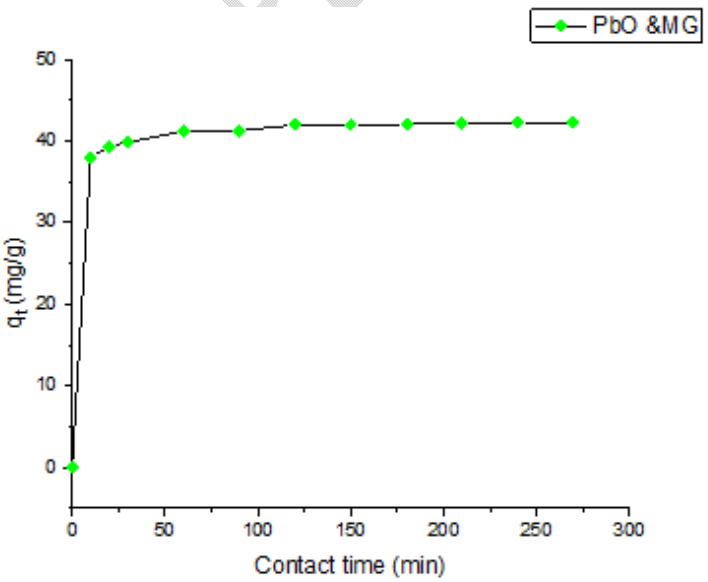

Figure (6): Adsorption capacity of PbO at different contact time

Conclusion:

The PbO-NPs is one of the most industrially used metal nanoparticles. Throughout this study, lead oxide nanoparticle was synthesized successfully by sol-gel method in a facile, cheap, and nontoxic way. SEM, EDX, XRD, BET analysis and FTIR-Spectroscopy characterization technique confirm the result. The crystalline nature and presence of PbO nanoparticle was confirmed from XRD and FTIR. The formation was supported by SEM images with the diameter of 22.4- 29.2 nm. The adsorption study illustrates the applicability and effectiveness of PbO nanoparticles as a sorbent for removing of MG dye. The results revealed that the adsorption of MG dye was relatively rapid as it attained equilibrium in 60 min with adsorption capacity of 41.3 mg. g^{-1}.

References:

1. Kumar, A., et al., *A rationalized and innovative perspective of nanotechnology and nanobiotechnology in chronic wound management*. 2020. **60**: p. 101930.
2. Nagpure, G., et al., *Nanobiotechnology for livestock breeding technologies*, in *Nanobiotechnology for the Livestock Industry*. 2023, Elsevier. p. 233-242.
3. Kuda, A. and M.J.M.T.P. Yadav, *Opportunities and challenges of using nanomaterials and nanotechnology in architecture: An overview*. 2022.
4. Abdin, A.R., A.R. El Bakery, and M.A.J.A.S.E.J. Mohamed, *The role of nanotechnology in improving the efficiency of energy use with a special reference to glass treated with nanotechnology in office buildings*. 2018. **9**(4): p. 2671-2682.
5. Bashir, S., et al., *Synergistic effects of doping, composite formation, and nanotechnology to enhance the photocatalytic activities of semiconductive materials*. 2023. **135**: p. 113264.
6. Kuiken, T., et al., *Public's Understanding, Perceptions, and Acceptance of Nanotechnology through the Lens of Consumer Products*, in *Nanoengineering*. 2015, Elsevier. p. 151-171.
7. Liu, Q., et al., *Physicochemical and in vitro digestion properties of soy isoflavones loaded whey protein nanoparticles using a pH-driven method*. 2022. **82**: p. 103209.

8. Erfani, A., M.K. Pirouzifard, and S.J.F.C. Pirsa, *Photochromic biodegradable film based on polyvinyl alcohol modified with silver chloride nanoparticles and spirulina; Investigation of physicochemical, antimicrobial and optical properties.* 2023: p. 135459.
9. Liu, Q., et al., *Physicochemical properties of nanoparticles affecting their fate and the physiological function of pulmonary surfactants.* 2021.
10. Huang, Y., et al., *Improving kidney targeting: The influence of nanoparticle physicochemical properties on kidney interactions.* 2021. **334**: p. 127-137.
11. Alavi, M., et al., *Metal and metal oxide-based antiviral nanoparticles: Properties, mechanisms of action, and applications.* 2022: p. 102726.
12. Ahmad, S., et al., *Diverse comparative studies for preferential binding of graphene oxide and transition metal oxide nanoparticles.* 2022. **647**: p. 129057.
13. Patil, S.P., R.Y. Chaudhari, and M.S.J.T.O. Nemade, *Azadirachta indica leaves mediated green synthesis of metal oxide nanoparticles: A review.* 2022: p. 100083.
14. Tao, D., et al., *PbO nanoparticles anchored on reduced graphene oxide for enhanced cycle life of lead-carbon battery*. 2022. **432**: p. 141228.
15. Mehrabi, N., et al., *Application of deep eutectic solvent for conjugation of magnetic nanoparticles onto graphene oxide for lead (II) and methylene blue removal.* 2020. **8**(5): p. 104222.
16. Bratovcic, A.J.L.C., *Synthesis, characterization, applications, and toxicity of lead oxide nanoparticles.* 2020. **6**: p. 66.
17. Soltanian, S., et al., *Biosynthesis of zinc oxide nanoparticles using hertia intermedia and evaluation of its cytotoxic and antimicrobial activities.* 2021. **11**: p. 245-255.
18. Kumar, N., et al., *TiO 2 and its composites as promising biomaterials: a review.* 2018. **31**: p. 147-159.
19. Miri, A., et al., *Biosynthesis and cytotoxic activity of lead oxide nanoparticles.* 2018. **11**(4): p. 567-572.
20. Kelaidis, N., et al., *Vapor–liquid–solid growth and properties of one dimensional PbO and PbO/SnO 2 nanowires.* 2022. **3**(3): p. 1695-1702.
21. Elawam, S., et al., *Characterizations of beta-lead oxide "massicot" nano-particles.* 2016. **17**(1): p. 1-10.

22. Noukelag, S., et al., *Bio-inspired synthesis of PbO nanoparticles (NPs) via an aqueous extract of Rosmarinus officinalis (rosemary) leaves.* 2021. **36**: p. 421-426.
23. Ranjbar, M. and M. Yousefi, *Sonochemical synthesis and characterization of a nano-sized lead (II) coordination polymer; a new precursor for the preparation of PbO nanoparticles.* 2016.
24. Mahmoud, M.E., et al., *Design and testing of high-density polyethylene nanocomposites filled with lead oxide micro-and nano-particles: Mechanical, thermal, and morphological properties.* 2019. **136**(31): p. 47812.
25. Marouzi, S., Z. Sabouri, and M.J.C.I. Darroudi, *Greener synthesis and medical applications of metal oxide nanoparticles.* 2021. **47**(14): p. 19632-19650.
26. Nafees, M., M. Ikram, and S.J.A.N. Ali, *Thermal stability of lead sulfide and lead oxide nano-crystalline materials.* 2017. **7**: p. 399-406.
27. Akay, D., U. Gökmen, and S.B.J.P.S. Ocak, *Structural role of double layer amphoteric oxides forms on electrical conductivity: PbO/zinc oxide semiconductor.* 2022. **97**(9): p. 095803.
28. Darki, S.Y., et al., *Effects of PVP surfactant and different alkalis on the properties of PbO nanostructures.* 2021. **262**: p. 124305.
29. Bouafia, A. and S.E.J.M.-R.i.O.C. Laouini, *Plant-mediated synthesis of iron oxide nanoparticles and evaluation of the antimicrobial activity: a review.* 2021. **18**(6): p. 725-734.
30. El Shafey, A.M.J.G.P. and Synthesis, *Green synthesis of metal and metal oxide nanoparticles from plant leaf extracts and their applications: A review.* 2020. **9**(1): p. 304-339.
31. Trivedi, R., et al., *Recent Advancements in Plant-Derived Nanomaterials Research for Biomedical Applications.* 2022. **10**(2): p. 338.
32. OSMAN, A.F., et al., *CHARACTERIZATION OF LEAD OXIDE MILLED NANOPARTICLES AND THE EFFECT OF THEIR INCORPORATION ON THE THERMAL PROPERTIES OF POLYSTYRENE.* 2023. **18**(1): p. 481-507.